Micro-CT imaging in species description: exploring beyond sclerotized structures in lichen moths (Lepidoptera: Erebidae, Arctiinae, Lithosiini) (#79790)

First submission

Guidance from your Editor

Please submit by **20 Jan 2023** for the benefit of the authors (and your token reward) .

Structure and Criteria
Please read the 'Structure and Criteria' page for general guidance.

Custom checks
Make sure you include the custom checks shown below, in your review.

Author notes
Have you read the author notes on the guidance page?

Raw data check
Review the raw data.

Image check
Check that figures and images have not been inappropriately manipulated.

Privacy reminder: If uploading an annotated PDF, remove identifiable information to remain anonymous.

Files

Download and review all files from the materials page.

7 Figure file(s)
4 Video file(s)
1 Raw data file(s)

Custom checks

DNA data checks

- Have you checked the authors data deposition statement?
- Can you access the deposited data?
- Has the data been deposited correctly?
- Is the deposition information noted in the manuscript?

New species checks

- Have you checked our new species policies?
- Do you agree that it is a new species?
- Is it correctly described e.g. meets ICZN standard?

Structure and Criteria

Structure your review

The review form is divided into 5 sections. Please consider these when composing your review:

1. **BASIC REPORTING**
2. **EXPERIMENTAL DESIGN**
3. **VALIDITY OF THE FINDINGS**
4. General comments
5. Confidential notes to the editor

You can also annotate this PDF and upload it as part of your review

When ready submit online.

Editorial Criteria

Use these criteria points to structure your review. The full detailed editorial criteria is on your guidance page.

BASIC REPORTING

- Clear, unambiguous, professional English language used throughout.
- Intro & background to show context. Literature well referenced & relevant.
- Structure conforms to PeerJ standards, discipline norm, or improved for clarity.
- Figures are relevant, high quality, well labelled & described.
- Raw data supplied (see PeerJ policy).

EXPERIMENTAL DESIGN

- Original primary research within Scope of the journal.
- Research question well defined, relevant & meaningful. It is stated how the research fills an identified knowledge gap.
- Rigorous investigation performed to a high technical & ethical standard.
- Methods described with sufficient detail & information to replicate.

VALIDITY OF THE FINDINGS

- Impact and novelty not assessed. *Meaningful* replication encouraged where rationale & benefit to literature is clearly stated.
- All underlying data have been provided; they are robust, statistically sound, & controlled.
- Conclusions are well stated, linked to original research question & limited to supporting results.

Standout reviewing tips

The best reviewers use these techniques

Tip	*Example*
Support criticisms with evidence from the text or from other sources	*Smith et al (J of Methodology, 2005, V3, pp 123) have shown that the analysis you use in Lines 241-250 is not the most appropriate for this situation. Please explain why you used this method.*
Give specific suggestions on how to improve the manuscript	*Your introduction needs more detail. I suggest that you improve the description at lines 57- 86 to provide more justification for your study (specifically, you should expand upon the knowledge gap being filled).*
Comment on language and grammar issues	*The English language should be improved to ensure that an international audience can clearly understand your text. Some examples where the language could be improved include lines 23, 77, 121, 128 – the current phrasing makes comprehension difficult. I suggest you have a colleague who is proficient in English and familiar with the subject matter review your manuscript, or contact a professional editing service.*
Organize by importance of the issues, and number your points	*1. Your most important issue* *2. The next most important item* *3. …* *4. The least important points*
Please provide constructive criticism, and avoid personal opinions	*I thank you for providing the raw data, however your supplemental files need more descriptive metadata identifiers to be useful to future readers. Although your results are compelling, the data analysis should be improved in the following ways: AA, BB, CC*
Comment on strengths (as well as weaknesses) of the manuscript	*I commend the authors for their extensive data set, compiled over many years of detailed fieldwork. In addition, the manuscript is clearly written in professional, unambiguous language. If there is a weakness, it is in the statistical analysis (as I have noted above) which should be improved upon before Acceptance.*

Micro-CT imaging in species description: exploring beyond sclerotized structures in lichen moths (Lepidoptera: Erebidae, Arctiinae, Lithosiini)

Simeão S Moraes [Corresp., 1], **Max S Söderholm** [2], **Tamara M. C. Aguiar** [1], **André V. L. Freitas** [1], **Pasi Sihvonen** [2]

[1] Biologia Animal, Universidade Estadual de Campinas, Campinas, Brazil

[2] Finnish Museum of Natural History, University of Helsinki, Helsinki, Finland

Corresponding Author: Simeão S Moraes
Email address: simeao_moraes@yahoo.com.br

X-ray micro-computed tomography imaging (micro-CT) is valuable for systematic research since it permits the non-destructive scanning and imaging of internal structures of very rare species and/or type specimens. Additionally, micro-CT allows to view the morphology and the functional anatomy of structures in their natural anatomical position, without deformations that typically occur using classical dissection protocols. In this study we provide the description of two new species of lichen moths (Lepidoptera: Erebidae, Lithosiini) from the Atlantic Forest in eastern Brazil: *Nodozana heliae* Moraes **sp. nov.** from Rio de Janeiro state and *Epeiromulona pataxo* Moraes & Aguiar **sp. nov.** from Bahia state. The male and female genitalia as well as the wing morphology were examined by means of non-destructive micro-CT, subsequent 3D model reconstruction, 360 degree spinning animations, 2D images from different angles, and those were compared against classical genitalia dissections from the same specimens. We conclude that techniques complement each other, micro-CT being particularly useful to study wing venation, sclerotized internal structures and muscles, while classical dissection is useful to study membranous structures, particularly in the female genitalia, abdominal skin and specialised scales on the male 8th sternite.

Micro-CT imaging in species description: exploring beyond sclerotized structures in lichen moths (Lepidoptera: Erebidae, Arctiinae, Lithosiini)

Simeão de Souza Moraes[1], Max Salvador Söderholm[2], Tamara Moreira Costa Aguiar[1], André Victor Lucci Freitas[1], & Pasi Sihvonen[2]

[1] Departamento de Biologia Animal and Museu de Zoologia, Universidade Estadual de Campinas, Campinas, Brazil

[2] Finnish Museum of Natural History "Luomus", University of Helsinki, Helsinki, Finland.

[*]Corresponding author:
Simeão Moraes
Rua Monteiro Lobato 255, Campinas, São Paulo, CEP 13083-862, Brazil
Email address: *simeao_moraes@yahoo.com.br*

Abstract

X-ray micro-computed tomography imaging (micro-CT) is valuable for systematic research since it permits the non-destructive scanning and imaging of internal structures of very rare species and/or type specimens. Additionally, micro-CT allows to view the morphology and the functional anatomy of structures in their natural anatomical position, without deformations that typically occur using classical dissection protocols.

In this study we provide the description of two new species of lichen moths (Lepidoptera: Erebidae, Lithosiini) from the Atlantic Forest in eastern Brazil: *Nodozana heliae* Moraes **sp. nov.** from Rio de Janeiro state and *Epeiromulona pataxo* Moraes & Aguiar **sp. nov.** from Bahia state. The male and female genitalia as well as the wing morphology were examined by means of non-destructive micro-CT, subsequent 3D model reconstruction, 360 degree spinning animations, 2D images from different angles, and those were compared against classical genitalia dissections from the same specimens. We conclude that techniques complement each other, micro-CT being particularly useful to study wing venation, sclerotized internal structures and muscles, while classical dissection is useful to study membranous structures, particularly in the female genitalia, abdominal skin and specialised scales on the male 8th sternite.

Keywords: integrative taxonomy, x-ray micro-computed tomography, morphology, muscles, dna barcode.

Introduction

Lepidoptera, commonly called butterflies and moths (or buttermoths), are covered with scales. The scales form a wide variety of diagnostic colors and patterns, particularly on wings but also on other body parts, and for that reason they are extensively used in Lepidoptera systematics. The scales also hide many structural details, which are important in systematics. These include for instance wing venation, which are particularly important in suprageneric classification, and modifications on the abdomen such as setae, spikes, modified sclerites and secondary sexual characters including the eversible scent-producing coremata (Scoble 1995, Kristensen 1999, Kristensen 2003). Other internal structures, which are important in systematics, include the reproductive organs and sclerites of thorax ~~and metathorax~~, to mention a few. These hidden structures have traditionally been studied by using various dissection techniques, the most requiring at least partial destruction (e.g. Hardwick 1950, Sihvonen 2001, Moraes & Duarte 2009, Murillo-Ramos *et al*. 2016). Also, learning of these dissection techniques requires extensive training and only some experts can master this "craftsmanship" in such detail that museums allow the dissection of their valuable type or rare specimens.

As regards the genitalia, the dissection techniques such as potassium hydroxide (KOH) treatment (Robinson 1976), if carefully applied and structures cleaned, reveal the sclerotized structures very well and those can be studied and imaged to the finest detail. The genitalia also contain membranous structures, and those are more difficult to study because those are transparent, delicate and easily break or are detached from other structures during the dissection. This is the case particularly in the female genitalia, and a notable problem with the KOH treatment is that it easily dissolves the male deposited spermatophores and female eggs inside the ovaries, or makes the muscles invisible, which means that important taxonomic information is lost. Staining enhances the study of the membranous structures, but still the problem remains that

classical dissection methods damage some structures, and certain structures are even removed routinely to make other structures visible. Finally, dissected structures are routinely embedded in microscopic slides and mounted in artificial position such as the male valvae spread out, or in some moth groups the male genitalia are unrolled (e.g Pitkin 1986), and the vesica is left uneverted inside the aedeagus. Some of these practises are useful for taxonomic research and for storage of extensive materials in museums, but it does not allow the subsequent study of the structures from various angles, which are important both in taxonomy and in functional anatomy research.

The X-ray micro-computed tomography imaging (micro-CT) is a fast and non-destructive data acquisition technique, which can complement the above-mentioned traditional, partly desctructive dissection methods, in morphological studies. Since its first application in entomology, 20 years ago (Hörnschemeyer *et al.* 2002), micro-CT is still relatively little used in insect morphology, mainly because the equipment is expensive and relatively few museums have it. The inspiring examples of micro-CT in Lepidoptera taxonomy include, among others, virtual dissections of reproductive organs (Simonsen & Kitching 2014), wing venation study on over 200-hundred-year-old type specimen (Robinson *et al*. 2018) and functional morphology of internal structures (Nath & Kunte 2020). Other benefits of the approach include the study of structures in their natural position without deformations, versatile post processing of data (Garcia *et al*. 2017a), and valuable material such as type specimens or rare species can be studied without damaging the samples (Stoev *et al*. 2013, Garcia *et al*. 2017b).

Lithosiini, popularly known as Lichen moths, is a species rich insect lineage whose subtribes and genus taxonomy are notorious, needing a modern integrative approach. The tribe includes approximately 3150 species, classified in 457 genera (Scott *et al*. 2014). Of these, 345

genera are classified as *incertae sedis* (Bendib & Minet 1999), and new species are described constantly (e.g. Durante & Apinda-Legnouo 2022, Volynkin *et al*. 2022a, b). The tribe is especially species-rich in the Neotropical region (Scott *et al*. 2018) and in Brazil, there are 212 species classified in 52 genera (Moraes & Casagrande 2019). However, these numbers are underestimated given the scarcity of specialists working with Neotropical fauna and the potential existence of new records and species.

While the morphology of Lithosiini moths have been studied extensively using classical methods, these moths have not been the target of micro-CT imaging earlier. We chose two undescribed lichen moth species as our study species. These originate from the Brazilian Atlantic Forest, which is one of the Earth's Biodiversity hotspots with high levels of diversity and endemism. The biodiversity and biomass in this area has been reported to be eroding in an alarming rate (de Lima *et al.* 2020). We aim to explore how micro-CT imaging can enhance the study of morphological structures compared to classical dissections and how it can be applied in systematic research. Our study focuses on structures that are not directly visible (scale-covered wing venation and abdominal structures) and on internal structures (genitalia) *in situ*, and finally, to conclude which of the two approaches (classical dissection and subsequent imaging or micro-CT imaging) is better suited for imaging different structures.

Material and Methods

Abbreviations

MZUSP	Museu de Zoologia da Universidade de São Paulo, Brazil
ZMH	Finnish Museum of Natural History, University of Helsinki, Finland
ZUEC	Zoological collection, Museu de Diversidade Biológica, Universidade Estadual de Campinas, Brazil

128

129 *Sampling and identification*

130 Moth sampling was carried out in Brazilian states Rio de Janeiro and Bahia between
131 2016–2021 during the new-moon phase to enhance light attractiveness using a 500 W mixed
132 light bulb and a white 2 m x 2 m sheet to attract the moths. Specimens were individually kept
133 alive in small glass containers, and those were killed with ethyl acetate immediately before the
134 wing spreading.

135 For identification, specimens were compared against relevant literature and online
136 sources (Seitz 1914, 1943, taxonomy section on Barcode of Life Data Systems
137 https://v4.boldsystems.org/), to material in relevant collections (ZUEC, MZUSP, ZMH),
138 including both type and non-type specimens, and DNA barcodes (658 bp region near the 5'
139 terminus of the COI mitochondrial gene) were compared against the genetic material available
140 on BOLD (Ratnasingham and Hebert 2007, 2013) and GenBank (Benson *et al*. 2013). Genetic
141 divergences between sequences were calculated using the number of base differences between
142 sequences. Voucher specimens are deposited at the above-mentioned institutions (details are
143 given under *Species description* chapter).

144

145 *DNA extraction and PCR protocol*

146 Three legs were removed from each specimen shortly after collection and before
147 spreading. Sampled legs were preserved dry and stored in 1.5 ml tubes at - 20˚ C. Total genomic
148 DNA was extracted with QIAcube DNA extraction robot (Qiagen, Netherlands) using DNeasy
149 Blood & Tissue Kit standard protocol with final elution in 100 µl elution buffer. The 5' end
150 (barcode region) of the mitochondrial gene cytochrome oxidase subunit I (COI, 650 bp) was

amplified for SSM3 sample with LepF1 (Wilson, 2012) and HCO (Folmer *et al.* 1994) primers. The barcode for SSM4 sample was amplified in two parts: the first half (~330bp) with LepF1 and mLepR1 (Wilson, 2012) primers and the end half (~450bp) with Beet (Simon *et al*. 1994) and HCO (Folmer *et al.* 1994) primers.

Polymerase chain reactions (PCRs) were performed with 13 µl total volume containing 3 µl of extracted DNA, 2 µl of H_2O milli-Q, 6.5 µl of 2x MyTaq HS red mix (Bioline Co., UK), and 0.75 µl of each primer (10 mM). PCR products were amplified as follows: 96˚C for 7 minutes, followed by 40 cycles of 96˚C for 30 seconds, 50˚C for 30 seconds and 72˚C for 90 seconds, and a final extension period of 72˚C for 10 minutes.

Amplicons were purified by mixing 5 µl of PCR product with 2 µl of 1/10 H_2O milli-Q diluted ExoSAP-IT (Thermofisher Scientific, USA). Purification was run in PCR machine: 37˚C for 15 min and 80˚C for 15 min. Purified products were sent for Sanger sequencing to FIMM (Institute for Molecular Medicine Finland).

Morphological examination

We first imaged the adult specimens using non-destructive micro-CT approach and tried to identify external and internal morphological structures *in situ*. Following this, both male and female abdomen and genitalia of both new species were dissected. When data from both approaches were available, this allowed to refine homology interpretations in both approaches.

Micro-CT imaging. Each adult specimen was pinned using minute pin, attached to a foam cube, which was traversed by standard insect pin. In order to avoid noise and artefacts resulting from the standard insect pin holding the foam cube, the pin was pushed down to exclude it from the scanning area. The samples were imaged using Nikon XT H 225 micro-

174 computed tomography. Scans were performed using multi-metal target with molybdenum
175 setting, with 73-74 kV beam energy, 94-95 uA beam current, 500 ms exposure time and 4476
176 projections with 4 frames per projection. Detector binning was set to 1x1 and gain to 24 dB.
177 Imaging was conducted using limited dynamic range after performing comparisons that showed
178 no visible differences between the longer full dynamic range scans and the faster limited
179 dynamic range scans. Effective pixel size ranged from 3.27 to 7.27 µm between the scans.
180 Projections were processed using Nikon CT pro 3D, and the 3D models were exported to
181 VGSTUDIO 3.5.2 (Volume Graphics GmbH, Heidelberg, Germany) in 16-bit. The 3D models
182 were visualized using two renderer modes, volume renderer (Phong) and X-ray, and they were
183 pseudo-colored to visualize density. Virtual section stacks in the three principal planes (coronal,
184 sagittal and axial) were exported in JPG format.
185 The external morphology and color pattern were analyzed following usual protocols
186 (Winter 2000).
187 **Dissection**. Abdomens and genitalia of females and males were dissected following
188 standard methods (Hardwick, 1950). The male aedeagus is shown both with uneverted vesica, to
189 allow comparison with older literature, and with everted vesica. The vesica was everted via the
190 caecum that was cut open by placing the aedeagus inside a hypodermic syringe (Sihvonen,
191 2001). Some structures were photographed during dissection *in situ* to allow an optimal angle for
192 observing and illustrating certain structures. Numerous dissected structures shown in the plates
193 were photographed in two to six images at different depths of focus, using a Leica DM1000
194 microscope and Leica DFC295 camera, and combined into single images using image-stacking
195 software in Adobe Photoshop CC v.20.0. For interpretation and descriptions of the genitalia
196 structures we followed the procedures outlined in Moraes & Duarte (2015), and terminology of

the male genitalia follows (Pierce 1909, Sibatani *et al.* 1954, Okagaki *et al.* 1955, Klots 1956, Ogata *et al.* 1957, Birket-Smith 1974) and female genitalia follows (Pierce 1914, Klots 1956, Mutuura 1972, Galicia *et al.* 2008). The muscle nomenclature follows Kuznetzov *et al*. (2004).

A total of 19 specimens belonging to the two new especies were examined, details are given under each species below.

The electronic version of this article in Portable Document Format (PDF) will represent a published work according to the International Commission on Zoological Nomenclature (ICZN), and hence the new names contained in the electronic version are effectively published under that Code from the electronic edition alone. This published work and the nomenclatural acts it contains have been registered in ZooBank, the online registration system for the ICZN (urn:lsid:zoobank.org:pub:68906FAC-208D-48D7-B69C-4ABDE6CFA0D6, urn:lsid:zoobank.org:act:F97C4D7C-65A3-4EEC-8D34-F84D5C7346EE, urn:lsid:zoobank.org:act:D4637E11-169E-45D0-8A25-6A61F68939A5). The ZooBank LSIDs (Life Science Identifiers) can be resolved and the associated information viewed through any standard web browser by appending the LSID to the prefix http://zoobank.org/. The online version of this work is archived and available from the following digital repositories: PeerJ, PubMed Central and CLOCKSS.

Results

Micro-CT imaging

The micro-CT scanning and post processing of 3D models allowed us to visualize clearly and in a non-destructive manner the wing venation and wing folds in both sexes (2D image in Fig. 1, 3D spinning video on Supplementary material 1), several sclerotized structures in the male abdomen, and several scleroritised structures and muscles in the male genitalia (Fig. 6).

The clearly visible male structures include, for instance, the posterior margin of the 8th abdominal tergite, tegumen, uncus, valva, transtilla, aedeagus and cornuti (2D image in Fig. 6, 3D spinning video on Supplementary material 2).

Non-sclerotized genital muscles were clearly visible in the 3D models (Fig. 6, Supplementary material 2). Those include

- m1 muscle. The depressor of uncus is a broad longitudinal muscle extending ventromedially from the anterior margin of tegumen to the base of uncus.
- m5 (7) muscle. The flexor of clasper is an intravalval muscle extending from the anterior part of the valva, in the region of sacculus, to the central part of valva. These muscles bend the valvae transversally, clasping the female abdomen during the copulation.
- m6 (5) muscle. The protractors of aedeagus originate on the dorsolateral region of the vinculum and insert on the base of the aedeagus.
- m7 (6) muscle. The retractors of aedeagus extend from the saccus and inserts mid-ventrally on the aedeagus.

As regards the membranous structures embedded in the abdomen, micro-CT scanning and post processing of 3D did not produce clear images and homology interpretation was difficult. This was mainly because the density of membranous structures and body fat were similar. As regards the female genitalia, which are mostly membranous, majority of the structures could be identified only via the sequential study of the sagittal slices (Supplementary material 3, 4). In the sagittal slices we were able to detect the sclerotized signa, antrum, and ductus bursae, which we used as reliable morphological anchor points, and subsequently from these images it was possible to infer the outer surface of the membranous corpus bursae and

ductus bursae (Fig. 7). By carefully adjusting the 3D histogram it was possible to identify further regions with very low density, representing the interior of the corpus bursae, membranous ducts, and margins of the pheromone glands (Fig 7).

Micro-CT imaging cannot be used to study the shape of eversible membranous structures. Among these is the male vesica, which we studied using the method of Sihvonen (2001), and we illustrated it to be morphologically complex in both studies species.

Species description

Comparison of our material, using both morphological and DNA barcode data, against described species of Lithosiini did not result in a positive match, thus suggesting our specimens belong to undescribed species. We provide the formal descriptions below.

Nodozana heliae Moraes **sp.nov.** (Figs. 1-3, 7)

Diagnosis (♂ and ♀). Prothoracic collar orange. Dorsal surface of forewing with several subrectangular white maculae, orange maculae on the wing base seahorse-shaped, orange maculae on the submarginal region hammer-shaped with an elliptical black spot inside. Compared with other *Nodozana* species, the wing pattern with white squares is idiosyncratic. Only *Nodozana toulgoeti* Gibeaux, 1983 has similar wing pattern, but without the red basal macula on the forewing. We combine taxon *heliae* to *Nodozana*, based on DNA barcode data (see below) and similar wing pattern with *N. toulgoeti*, but highlight that genus-level systematics of Neotropical lichen moths are poorly resolved and more research is needed. *N. toulgoeti* is known from French Guiana.

Description (♂ and ♀). Head. Brown. Frons brown, vertex yellow. Labial palp brown. **Thorax**. Predominantly brown. Prothoracic collar orange; prothoracic coxa brown. Tegulae beige. **Wings**: Venation as in Figure 1b: Wingspan 15,5–17,5 mm (n=4). Forewing backgound

dark brown; basal orange seahorse-shaped macula; white subrectangular maculae distributed on post-basal, discal, post-discal and marginal regions; post-discal region with orange hammer-shaped maculae between M_1 and CuP veins; elliptical black macula between M_1 and M_3; ventral surface of forewing dark brown, with narrow orange stripe near wing apex; maculae obscured by dark brown scales. Hindwing yellow, apex with dark brown macula, outer margin outlined by dark brown scales; ventral surface similar. **Abdomen**. Dorsally light brown, posterior margin of segments A_2-A_8 outlined by dark brow scales; ventrally similar. 7^{th} sternite margins weakly sclerotized, posterior margin concave. 8^{th} sternite with anterior and lateral margins sclerotized, setose coremata medially. **Male Genitalia**: Tegumen trapezoidal in dorsal view, anterior margin concave. Uncus hooked, apex acute. Valva entire, sub-rectangular; sacculus developed, fold on inner surface, oriented towards distal-medial axis. Transtilla sclerotized, inverted U shaped. Juxta membranous. Subscaphium sclerotized. Aedeagus rectilinear, sclerotized, with micro spicules on anterior portion near vesica; caecum rounded, foramen lateral; vesica large, with three large diverticula, single spiniform cornutus. **Female Genitalia**. Seventh sternite smooth. Ostium membranous. Antrum sclerotized, with microspicules. Ductus bursae short, membranous. Corpus bursae extending beyond seventh sternite, signa as two patches of spines on lateral portion of bursa. Lamella antevaginalis and postvaginalis absent. Papillae anales narrow, setose.

Etymology. The specific epithet is granted in honor to Maria Hélia de Souza Moraes, mother of the first author. It is also a reference between the golden scales on the forewing with Helios, the personification of the sun in Greek mythology.

Distribution. The only record for this species is from Itatiaia, a montane dense ombrophilous forest of medium and high altitudes in the state of Rio de Janeiro, Brazil.

289 **DNA barcode data**. (n=1) from Brazil: Rio de Janeiro. Nearest lichen moth species,
290 based on nucleotide blast function on GenBank, is *Nodozana toulgoeti* from French Guiana with
291 7% difference.
292 **Type series**. HOLOTYPE ♀: BRAZIL: **Rio de Janeiro**: Itatiaia, Parque nacional do
293 Itatiaia, Alojamento 12, 01-04/viii/2016, Simeão Moraes, Tamara Aguiar, André Taciolli leg.,
294 label: LEPSM 551 (ZUEC). PARATYPES BRAZIL: 1♀ **Rio de Janeiro**: Itatiaia, Parque
295 nacional do Itatiaia, Alojamento 12, 01-04/viii/2016, Simeão Moraes, Tamara Aguiar, André
296 Taciolli leg., labels: Simeão Moraes Genitalia 516, LEPSM 1093 (ZUEC); 1♂ **Rio de Janeiro**:
297 Itatiaia, Parque nacional do Itatiaia, Casa do Pesquisador 12, 05-12/iv/2021, 22˚27'19.9''S
298 44˚36'29'' W, Simeão Moraes leg., labels: Pasi Sihvonen Prep. Number 2870, LEPSM 1382
299 (ZUEC); 1♀ **Rio de Janeiro**: Itatiaia, Parque nacional do Itatiaia, Casa pesquisador, 05-
300 12/iv/2021, 22°27'19.9''S 44.36'20.0''W, Simeão Moraes leg., labels: LEPSM 1439, SSM DNA
301 sample 3, specimen ID http://id.luomus.fi/GBT.11(ZMH).
302
303 *Epeiromulona pataxo* Moraes & Aguiar **sp.nov.** (Figs. 1, 4, 5)
304 **Diagnosis (**♂ and ♀**)**. Forewing dorsally white with several small black maculae on the
305 proximal portion, outer margin with reddish scales. Hindwing uniform salmon-colored. The
306 forewing pattern with white / beige background and black maculae / dots are shared with other
307 species in *Epeiromulona*, but the reddish outer margin is idiosyncratic in *Epeiromulona pataxo*.
308 **Description (**♂ and ♀**). Head**. White. Frons brown, vertex white. Labial palp white.
309 **Thorax**. Predominantly white. Prothoracic collar white; prothoracic coxa white. Tegulae white.
310 **Wings**: Venation as in Figure 1a. Wingspan 12,75–13,3mmmm (n=15). Forewing background
311 white withtwo proximal maculae: elliptical on costal margin, rounded on trunk of A vein; four

maculae on medial region: two elliptical on costal margin, subrectangular at discal cell, subretangular at A vein; submarginal region with two sinuous stripes, proximal longer than distal; outer margin with reddish scales; ventral surface reddish with black maculae fused along basal length of costal margin, black stripes fused on subapical region. Hindwing dorsally salmon-colored; ventrally salmon with apical black macula on region of Rs and M1. **Abdomen**. Dorsally salmon-colored on A_2-A_4, reddish on A_3-A_8; ventrally salmon. Male segments 7-8 not differentiated. **Male Genitalia**: Tegumen subrectangular in dorsal view, anterior margin concave. Uncus hooked, apex acute. Vinculum narrow. Valva rather immobile, setose, sub-triangular, apex rounded; sacculus developed, consisting of fold on inner surface, oriented towards distal-medial axis. Saccus large, subtriangular. Juxta sclerotized, subtriangular. Subscaphium smooth. Aedeagus rectilinear, sclerotized, two rows of spines on apex; ejaculatory bulb rounded, foramen lateral; vesica bilobated, cornuti on bigger lobe: micro spines medially and needle-shaped spines on distal part. **Female Genitalia**. **7th** sternite smooth. Ostium membranous. Antrum slightly sclerotized, smooth. Ductus bursae short, membranous. Corpus bursae massive, extending beyond the seventh sternite, with two patches of signa, spines on posterior portion, weakly fused micro spicules on anterior portion. Lamella antevaginalis and postvaginalis not sclerotized. Papillae anales large, setose.

Etymology. The specific epithet honors the Pataxós, indigenous people inhabiting the state of Bahia, Brazil, which is the location where the specimens were collected. A masculine name in apposition.

Distribution. The only record for this species is the National Park of Monte Pascoal, in Porto Seguro, State of Bahia, Brazil. The region represents one of the last remnants of the

Atlantic Forest, where the predominant vegetation is tropical rain forest, and the physiognomic and structural aspect is similar to the dense and exuberant vegetation of Amazonian Hileia.

DNA barcode data. (n=1) from Brazil: Bahia. Nearest species, based on nucleotide blast function on GenBank, is *Epeiromulona* sp. from Costa Rica with 7% difference.

Type series. HOLOTYPE ♂: BRAZIL: **Bahia**: Porto Seguro, Parque Nacional Monte Pascoal, Sede, 150m, 12-23/v/2021, 16˚53'16.13'' S 39˚24'57.46''W, Simeão Moraes leg., (ZUEC). PARATYPES BRAZIL: 1♀ **Bahia**: Porto Seguro, Parque Nacional Monte Pascoal, Sede, 150m, 12-23/v/2021, 16˚53'16.13'' S 39˚24'57.46''W, Simeão Moraes leg., (ZUEC); 7♂♂ **Bahia**: Porto Seguro, Parque Nacional Monte Pascoal, Sede, 150m, 12-23/v/2021, 16˚53'16.13'' S 39˚24'57.46''W, Simeão Moraes leg., (ZUEC); 2 ♂♂ **Bahia**: Porto Seguro, Parque Nacional Monte Pascoal, Sede, 150m, 12-23/v/2021, 16˚53'16.13'' S 39˚24'57.46''W, Simeão Moraes leg., (MZUSP); 2♂♂ **Bahia**: Porto Seguro, Parque Nacional Monte Pascoal, Sede, 150m, 12-23/v/2021, 16˚53'16.13'' S 39˚24'57.46''W, Simeão Moraes leg.. 1♂ **Bahia**: Porto Seguro, Parque Nacional Monte Pascoal, Sede, 150m, 12-23/v/2021, 16˚53'16.13'' S 39˚24'57.46''W, Simeão Moraes leg., Genitalia SSM A, specimen ID http://id.luomus.fi/GBT.12 (ZMH); 1♂ **Bahia**: Porto Seguro, Parque Nacional Monte Pascoal, Sede, 150m, 12-23/v/2021, 16˚53'16.13'' S 39˚24'57.46''W, Simeão Moraes leg., Pasi Sihvonen, prep. number 2868; Pasi Sihvonen, DNA sample 1544, specimen ID http://id.luomus.fi/GBT.13 (ZMH).

Discussion

The two species herein described have idiosyncratic wing patterns, both distinct from other lichen moth species occuring in Atlantic forest biome. Although the geographical distribution recorded is narrow, we expect that these species might be found in other areas in

similar habitats near Rio de Janeiro and Porto Seguro. These species may be have been overlooked because of their small size, and secondly, the specialists investigating the Neotropical fauna of lichen moths is almost non-existent.

Sclerotized and membranous structures

In Lepidoptera taxonomy, wing venation characters, in addition to abdomen and genitalia characters, are among the most diagnostic and those are routinely studied and illustrated in publications (e.g. Carter & Kristensen 1998, Winter 2000, Moraes & Duarte, 2009). However, because Lepidoptera are covered with scales, these characters cannot be studied without scale removal. The widely used protocols are partly destructive, such as wing bleaching that removes color from scales (e.g. Moraes & Duarte 2009, Murillo-Ramos *et al*. 2016), or KOH approach that dissolves body fat, but makes the sclerotized structures in the abdomen and genitalia visible (e.g. Hardwick, 1950, Robinson 1976). Although membranous structures may be visible to some degree after KOH treatment, their visualization also depend on the successful application of stains such as Chlorazol Black and Eosin. In these approaches, some membranous structures such as ducts, are routinely removed and other abdominal structures such as androconial scales and pheromone glands are rarely illustrated.

We noted that non-destructive micro-CT imaging and post processing of 3D models provided relatively easy and informative access to certain sclerotized and non-sclerotized structures. On the 3D wing models, it was possible to identify veins in detailed manner, and folds on the wing membrane close to the anal veins in both wings. Sometimes these folds are mistakenly identified as veins on 2D images. As regards the male genitalia, 3D models illustrated clearly majority of the sclerotized structures such as tegumen, uncus, transtilla, aedeagus and

valvae (Fig. 6). Non-sclerotized structures were difficult to visualize, including for instance membranous juxta in the male genitalia of *Nodozana heliae* Moraes sp. nov. and membranous structures in the female genitalia.

Muscles

Four ~~non-sclerotized~~ genital muscles were clearly visible in the 3D models (Fig. 6, Supplementary material 2): m1, m5 (7), m6 (5) and m7 (6). Because micro-CT models illustrate the structures in their natural position, it allowed inferring the precise origin and inserting regions of muscle fibers and their naming. For example, the anatomical position of the aedeagus on the genital capsule allowed the distinction between the protractor and retractor muscles of the aedeagus (m6 (5) and m7 (6)) (Figure 6). The former appears longer in length, with origin in the dorsomedial portion of the vinculum and insertion in the base of the aedeagus, close to the caecum; the latter set of muscles are shorter and originates in the most ventral portion of the vinculum (saccus) and inserts in the central-ventral portion of the aedeagus. We did not detect the presence of muscle m8 (3), which has its origin in the median part of the vinculum and inserts at the distal margin of the juxta, being an indirect abductor of the valvae (Kuznetzov *et al*. 2004). The absence of m8 (3) might be correlated with the absence of a sclerotized juxta in the *Nodozana heliae* Moraes sp. nov.

The abductor and adductor musculature of the valva m3 (2) and m4 were not clearly distinguished in the 3D models. Although it is possible to identify something similar to muscles in the region between the transtilla and the valva, a better rendering of the 3D models is necessary to accurately assess the presence of these muscles, as well as the retractor muscle of vesica (m21), usually located inside the base of aedeagus (Kuznetzov *et al*. 2004). In our study

species the valvae are morphologically simple, without all morphological subdivisions proposed by Sibatani *et al.* (1954), but we managed to identify the intravalval muscle m5 (7), the flexor of clasper. This indicates that it may be possible to identify more muscles in species with more complex valva, such as some lichen moths species in genus *Inopsis* Felder, 1874 in which it is possible to identify all six subdivisions of valva. Further, micro-CT approach may help to access the configuration of the intravalval musculature and to investigate whether the valva subunits have intrinsic musculature. This may provide new evidence on serial homology studies for the appendicular origin of the male genitalia, and allow evaluating plesiomorphic or derived characters in a phylogenetic context (Moraes 2014).

Classical approaches are superior for certain structures

The classical, partly destructive dissection methods we used allowed us to identify in better detail some membranous structures (Figs. 2-5). These include, for instance, the abdominal skin and specialized scales on the male 8th sternite(in *Nodozana heliae* Moraes sp. nov., the ductus ejaculatorius in males, and the ductus bursae, corpus bursae and papillae anales in females. Details of the male vesica, i.e. shape, size and position of sclerotized structures and membranous diverticula, were only visible in the classical approach (Sihvonen 2001) (Figs 2, 4). In lichen moths, the vesica has been shown to be rather complex and very informative for taxonomy, with some species showing several diverticula and different shapes of cornuti (Durante & Apinda-Legnouo 2022, Volynkin *et al*. 2022a, b). Our result support earlier view: also in the smallest lichen moths, the vesica is complex and contains diagnostic characters.

Conclusion

Our results demonstrate that micro-CT scanning combined with traditional dissection protocols can be used to create virtual dissections of the male genitalia in lichen moths, where the most of the diagnostic structures are clearly visible. Furthermore, 3D reconstructions have the advantage of visualizing the morphological structures, such as the genitalia muscles and wing venation, without scale removal. Muscle information is usually lost with the use of KOH and wing colors are lost if bleaching is used.

Although the 3D reconstruction presented here are very promising, we emphasize that micro-CT scanning cannot fully replace the abdomen and genitalia dissections in Lepidoptera for systematics and taxonomy purposes. Many specimens will not produce satisfactory 3D models, and membranous structures embedded inside soft tissue such as body fat, appear problematic. This is often the case for the female genitalia in Lepidoptera, where the genitalia are almost entirely internal and membranous, and as well as for some important traits in the male genitalia, such as the vesica. The shape and number of lobes of the latter can only be fully understood when the structure is physically everted and shown as maximally inflated. Wings are rather 2D structures and for the study of wing venation we recommend micro-CT scanning as the first approach. We also acknowledge that further post-image processing of raw data could allow identifying additional structures, which were not visible to us.

The advantages of using micro-CT in systematics are undeniable. First, it represents a non-destructive method that can be used to study the type specimens and/or rare species. Second, it has the potential to access information on the morphology and the functional anatomy of structures in their natural anatomical position, which otherwise would be deformed or lost with classical dissection protocols. The use of micro-CT offers new opportunities for enhancing

taxonomic descriptions and comparative studies, e.g via video files, broadening the utility of morphological characters also in other disciplines in biology.

ACKNOWLEDGEMENTS

Elina Laiho (Finnish Museum of Natural History, University of Helsinki) and Eduardo de Proença Barbosa are thanked for processing the DNA barcodes. The present study is registered in the SISGEN (A6751E2).

References

Alba-Tercedor J, Hunter WB & Alba-Alejandre I. 2021. Using micro-computed tomography to reveal the anatomy of adult *Diaphorina citri* Kuwayama (Insecta: Hemiptera, Liviidae) and how it pierces and feeds within a citrus leaf. *Scientific Reports* 11: 1358 (2021). https://doi.org/10.1038/s41598-020-80404-z.

Bendib A & Minet J. 1999. Lithosiine main lineages and their possible interrelationships. I. –Definition of new or resurrected tribes (Lepidoptera: Arctiidae). Annales de la Société Entomologique de France 35: 241–263.

Birket-Smith J. 1974. Morphology of the male genitalia of Lepidoptera I. Ditrysia. *Entomologica Scandinavica*, *5,* 1–22.

Carter DJ & Kristensen NP. 1998. Classification and Keys to Higher Taxa. Lepidoptera, Moths and Butterflies, pp. 27-49. Vol. 1. Part 35. Evolution, Systematics and Biogeography. In:Fischer, M. (ed.). Handbuch der Zoologie Band IV. Arthropoda: Insecta. Walter de Gruyter, Berlin, New York. 567 pp.

de Lima RAF, Oliveira AA & Pitta GR. 2020. The erosion of biodiversity and biomass in the Atlantic Forest biodiversity hotspot. *Nature Communications* **11**: 6347 (2020). https://doi.org/10.1038/s41467-020-20217-w

Donato S, Vommaro ML, Tromba G & Giglio A. 2021.Synchrotron X-ray phase

contrast micro tomography to explore the morphology of abdominal organs in Pterostichus melas italicus Dejean, 1828 (Coleoptera, Carabidae). *Arthropod Structure & Development* 62: 2021,101044.

Durante A & Apinda-Legnouo EA. 2022. Sixth contribution to the study of the Lithosiini of Gabon: the genus *Pseudopoliosia* Krüger, 2015 (Lepidoptera: Erebidae: Arctiinae). *Zootaxa, 5195*: 554-566.

Folmer O, Black M, Hoeh W, Lutz R & Vrijenhoek R. 1994. DNA primers for amplification of mitochondrial cytochrome c oxidase subunit I from diverse metazoan invertebrates. Molecular Marine Biology and Biotechnology 3: 294-299.

Galicia I, Sánchez V, & Cordeiro C. 2008. On the function of signa, a genital trait of female Lepidoptera. *Annals of the Entomological Society of America*, *101*, 786–793.

Garcia FH, Fischer G, Liu C, Audisio TL, Alpert GD, Fisher BL, Economo EP. 2017a. X-Ray microtomography for ant taxonomy: an exploration and case study with two new Terataner (Hymenoptera, Formicidae, Myrmicinae) species from Madagascar. *PLoS One* 12:1–36.

Garcia FH, Fischer G, Liu C, Audisio TL, Economo EP. 2017b. Next-generation morphological character discovery and evaluation: an X-ray micro-CT enhanced revision of the ant genus *Zasphinctus* Wheeler (Hymenoptera, Formicidae, Dorylinae) in the Afrotropics. *Zookeys* 23: 33-93.

Hardwick DF. 1950. Preparation of slide mounts of Lepidopterous genitalia. Canadian Entomologist 82:231–235.

Hörnschemeyer T, Beutel RG & Pasop F. 2002. Head structures of *Priacma serrata* Leconte (Coleptera, Archostemata) inferred from X-ray tomography. *Journal of Morphology* 252: 298–314. https://doi.org/10.1002/jmor.1107.

Klots AB. 1956. Lepidoptera. In: Tuxen LS, ed. *Taxonomist's glossary of genitalia in insects*. Copenhagen: Munksgaard, 97–110.

Kristensen NP (ed.) 1999: Handbook of Zoology, vol. 4 Artthropoda: Insecta, part 35: Lepidoptera, moths and butterflies. Volume 1: Evolution, systematics and biogeography. Walter de Gruyter, Berlin. 491 p.

Kristensen NP (ed.) 2003: Handbook of Zoology, vol. 4 Artthropoda: Insecta, part 36:

Lepidoptera, moths and butterflies. Volume 2: Morphology, physiology and development. Walter de Gruyter, Berlin. 564 p.

Kuznetzov VI, Speidel W, Naumann CM, Stekolnikov AA. 2004. The skeleton and musculature of male and female terminalia in *Oenosandra boisduvalii* Newman, 1856 and the phylogenetic position of the family Oenosandridae (Insecta: Lepidoptera). SHILAP Revista de lepidopterología 32: 297–313.

Moraes SS & Duarte M. 2009. Morfologia comparada das três espécies do complexo *Telchin licus* (Drury) (Lepidoptera, Castniidae) com uma sinonímia. *Revista Brasileira de Entomologia 53*: 245–265.

Moraes SS. 2014. Cladistic analysis of subtribe Pericopina and taxonomic revision of *Dysschema* Hübner, 1818 (Lepidoptera: Erebidae: Arctiinae: Arctiini). Doctoral Dissertation. Available at http://www.teses.usp.br/teses/disponiveis/41/41133/tde-11072014-103044/ptbr.php

Moraes SS & Duarte M. 2015. Description of four new species of tiger moth genus *Dysschema* Hübner (Lepidoptera: Erebidae, Arctiinae, Arctiini, Pericopina). *Zootaxa*, *4006*, 540–550.

Moraes SS, Casagrande MM. 2019. Lithosiini *in* Catálogo Taxonômico da Fauna do Brasil. PNUD. Available in: <http://fauna.jbrj.gov.br/fauna/faunadobrasil/173341>.

Morimoto J, Barcellos R, Schoborg TA, Nogueira LP & Colaço MV. 2022. Assessing Anatomical Changes in Male Reproductive Organs in Response to Larval Crowding Using Micro-computed Tomography Imaging. *Neotropical Entomology* 51: 526–535. https://doi.org/10.1007/s13744-022-00976-5.

Murillo-Ramos L, Hernández-Mejía C, Llorente- Bousquets J. 2016. The phylogenetic position of Aphrissa (Lepidoptera: Pieridae: Coliadinae) within its relatives the ancient American Catopsilias. Zootaxa 4147: 538–550.

Mutuura A. 1972. Morphology of the female terminalia in Lepidoptera, and its taxonomic significance. *Canadian Entomologist*,104, 1055–1071.

Nath BD, Kunte K. 2020: Tools of the trade: MicroCT reveals native structure and functional morphology of organs that drive caterpillar–ant interactions. Scientific Reports 10:10593 https://doi.org/10.1038/s41598-020-67486-5.

Ogata M, Okada Y, Okagaki H & Sibatani A. 1957. Male genitalia of Lepidoptera: morphology and nomenclature III. Appendages pertaining to the tenth somite. *Annals of the Entomological Society of America*, *50*, 237–244.

Okagaki H, Sibatani A, Ogata M & Okada Y. 1955. Male genitalia of Lepidoptera: morphology and nomenclature II. Morphological significance of sacculus and furca. *Annals of the Entomological Society of America*, *8*, 438–442.

Pierce FN. 1909. The genitalia of the group Noctuidae of the Lepidoptera of the British Islands. *An account of the morphology of the male clasping organs*. Liverpool: A. W. Duncan.

Pierce FN. 1914. The genitalia of the group Geometridae of the Lepidoptera of the British Islands. *An account of the morphology of the male clasping organs and the corresponding organs of the female*. Liverpool: A. W. Duncan.

Pitkin LM. 1986. A technique for the preparation of complex male genitalia in Microlepidoptera. Entomologist's Gazette, 37: 173-179.

Ratnasingham S, Hebert PDN. 2007. BOLD: The Barcode of Life Data System www. barcodinglife.org Molecular Ecology Notes. https://doi.org/10.1111/j.1471-8286.2007.01678.x

Ratnasingham S, Hebert PDN. 2013. A DNA-Based registry for all animal species: The Barcode Index Number (BIN) System. PLoS ONE 8(7): e66213. https://doi.org/10.1371/journal.pone.0066213.

Robinson GS. 1976: The preparation of slides of Lepidoptera with special reference to the Microlepidoptera. Entomologists's Gazetter 27: 127-132.

Robinson J, Gibson J, Arevalo-Maldonado HA, de Prins J, Windmill J. 2018. A non-destructive virtual dissection by micro-CT reveals diagnostic characters in the type specimen of *Caloptilia stigmatella* (Lepidoptera: Gracillariidae). Zootaxa 4441: 137-150.

Scoble MJ. 1995: The Lepidoptera: form, function and diversity. Natural History Museum, UK. 404 p.

Scott CH, Zaspel JM, Chialvo P, Weller J. 2014. A preliminary molecular phylogenetic assessment of the lichen moths (Lepidoptera: Erebidae: Arctiinae: Lithosiini) with comments on palatability and chemical sequestration *Systematic Entomology* 39: 286–303.

Seitz A. 1943. Les Macrolepidopteres du Globe. Tome XIV (Edition Française). Paris, 600 pp., 80 pls.

Seitz A. 1914. Subfamilie: Lithosiinae, Flechtenbärchen (partim): pp. 118-134. In: Seitz A, 1911-1933 – Die Gross-Schmetterlinge der Erde 10. Spinner und Schwärmer des indoautralischen Gebiets, Stuttgart: 909 pp., 100 pls.

569 Sibatani A, Ogata M, Okada Y & Okagaki H. 1954. Male genitalia of Lepidoptera: morphology
570 and nomenclature. I. Divisions of the valvae in Rhopalocera, Phalaenidae (= Noctuidae) and
571 Geometridae. *Annals of the Entomological Society of America*, 47, 93–106.
572 Sihvonen P. 2001. Everted vesicae of the *Timandra griseata* group: methodology and differential
573 features (Geometridae, Sterrhinae). Nota Lepidopterologica 24:57–64.
574 Simon C, Frati F, Beckenbach A, Crespi B, Liu H, Flook P. 1994. Evolution, Weighting, and
575 Phylogenetic Utility of Mitochondrial Gene Sequences and a Compilation of Conserved
576 Polymerase Chain Reaction Primers. *Annals of the Entomological Society of America 87(6)*:
577 651–701.
578 Simonsen TJ & Kitching IJ. 2014. Virtual dissections through micro-CT scanning:
579 a method for non-destructive genitalia 'dissections' of valuable Lepidoptera material.
580 *Systematic Entomology* 39: 606-618. https://doi.org/10.1111/syen.12067.
581 Stoev P, Komerički A, Akkari N, Liu S, Zhou X, Weigand AM, Hostens J, Hunter CI, Edmunds
582 SC, Porco D, Zapparoli M, Georgiev T, Mietchen D, Roberts D, Faulwetter S, Smith V,
583 Penev L. 2013. *Eupolybothrus cavernicolus* Komerički & Stoev sp. n. (Chilopoda:
584 Lithobiomorpha: Lithobiidae): the first eukaryotic species description combining
585 transcriptomic, DNA barcoding and micro-CT imaging data. *Biodiversity Data Journal* 28:
586 e1013. doi: 10.3897/BDJ.1.e1013.
587 Volynkin AV, Cerny K, Huang S-Y, Saldaitis A. 2022a. On the taxonomy of *Barsine striata*
588 (Bremer & Grey) and *Barsine pulchra* (Butler) (Lepidoptera: Erebidae: Arctiinae) with
589 descriptions of three new species from Indochina. *Zootaxa, 5175*: 253-274
590 Volynkin AV, Cerny K, de Vos R. 2022b. Two new species of the subgenus Cryptanaema de
591 Vos of the genus *Cyana* Walker from eastern Indonesia (Lepidoptera: Erebidae: Arctiinae:
592 Lithosiini: Nudariina). *Zootaxa, 5178*: 81-91.
593 Wilson JJ. 2012. DNA barcodes for insects. Methods in Molecular Biology 858:17-46.
594 Winter WD. 2000. Basic techniques for observing and studying moths and butterflies. *Memoirs*
595 *of the Lepidopterists' Society*, *5*, 1–444.
596 Wootton RJ. 1979. Function, homology and terminology in insect wings. *Systematic*
597 *Entomology, 4*: 81–93. DOI 10.1111/j.1365-3113.1979.tb00614.x.

Figure 1

General appearance of new described species and micro-CT images of wing venation

A. *Epeiromulona pataxo* Moraes & Aguiar **sp. nov**. B. *Nodozana heliae* Moraes **sp. nov.**

Venation terminology after Wootton (1979).

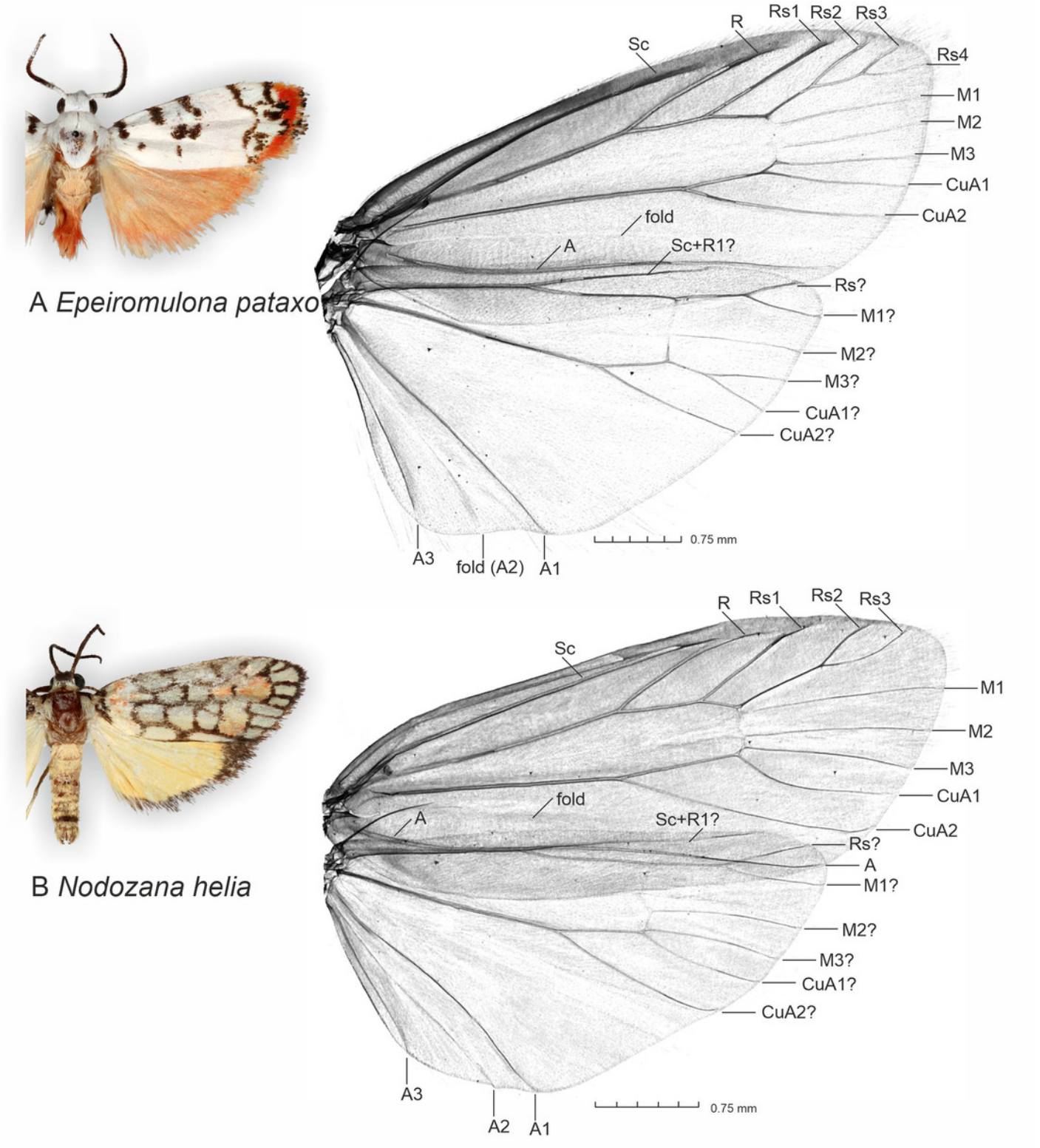

Figure 1. General appearance and micro-CT images of male wing venation. A. *Epeiromulona pataxo* Moraes & Aguiar sp. nov. B. *Nodozana helia* Moraes sp. nov. Venation terminology after Wootton (1979).

Figure 2

Habitus and male genitalia of *Nodozana heliae* Moraes sp. nov. (paratype)

A. Habitus, dorsal and ventral view, wingspan 16 mm. B. Genital capsule, ventral view. C. Aedeagus, ventral view. D. Aedeagus with everted vesica, lateral view. E. Detail of micro spicules at apex of aedeagus. F. 7th sternite and androconial scent organ associated to the 8th sternite. G. 8Th sternite with androconial scales removed.

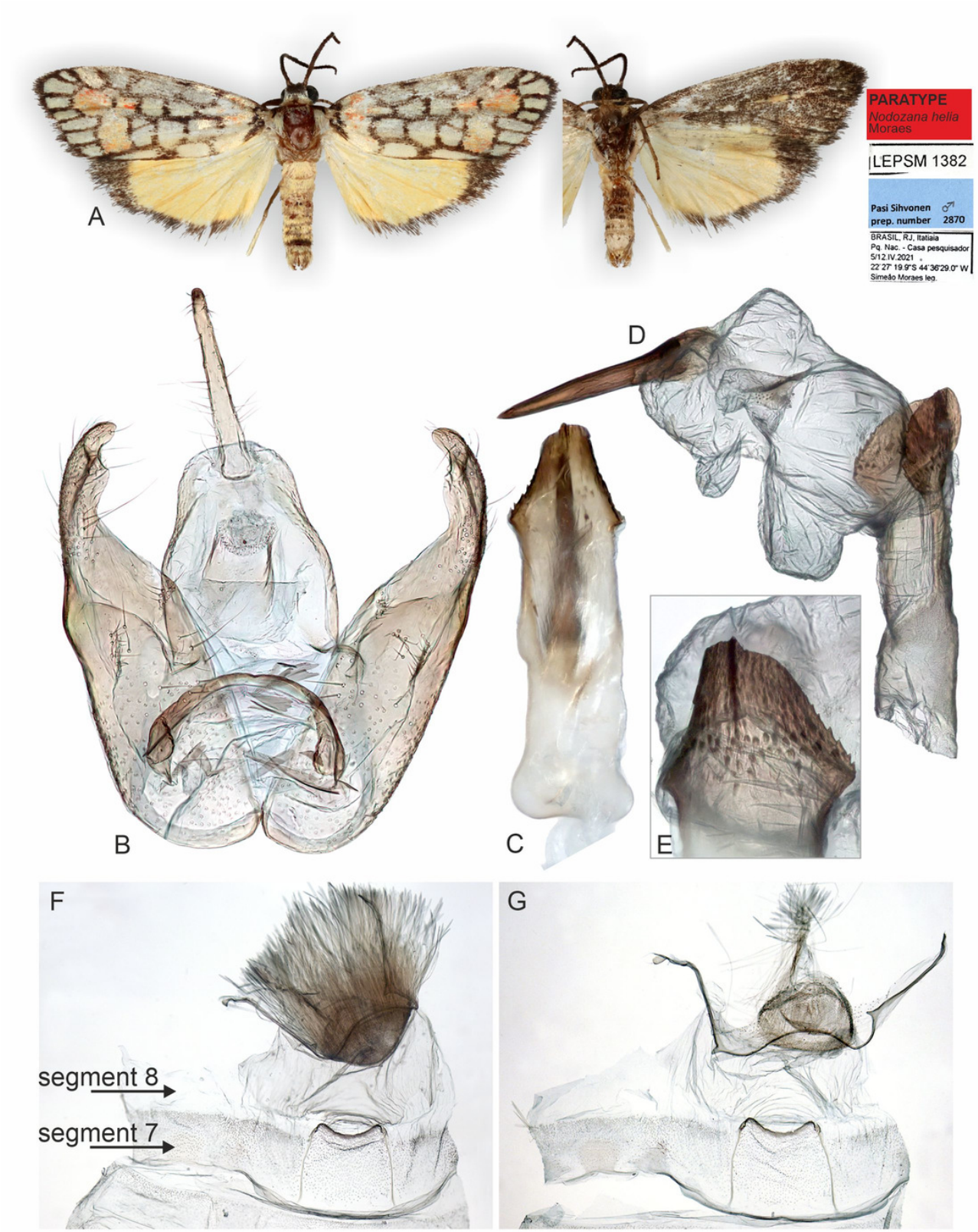

Figure 2. Habitus and male genitalia of *Nodozana helia* Moraes **sp. nov.** (paratype). A. habitus, dorsal and ventral view, wingspan 16 mm. B. Genital capsule, ventral view. C. Aedeagus, ventral view. D. Aedeagus with everted vesica, lateral view. E. Details of micro spicules at apex of aedeagus. F. 7th sternite and androconial scent organ associated to the 8th sternite. G. 8th sternite with androconial scales removed.

Figure 3

Habitus and female genitalia of *Nodozana heliae* Moraes sp. nov. (paratype)

A. Habitus, dorsal and ventral view, wingspan 18 mm. B. Female genitalia, ventral view, point of origin of ductus seminalis indicated with circle. C. Detail of pheromone gland, dorsal view. D. Detail of signum on posterior portion of corpus bursae. E. Detail of signum on anterior portion of corpus bursae. All pictures from dissection SSM516

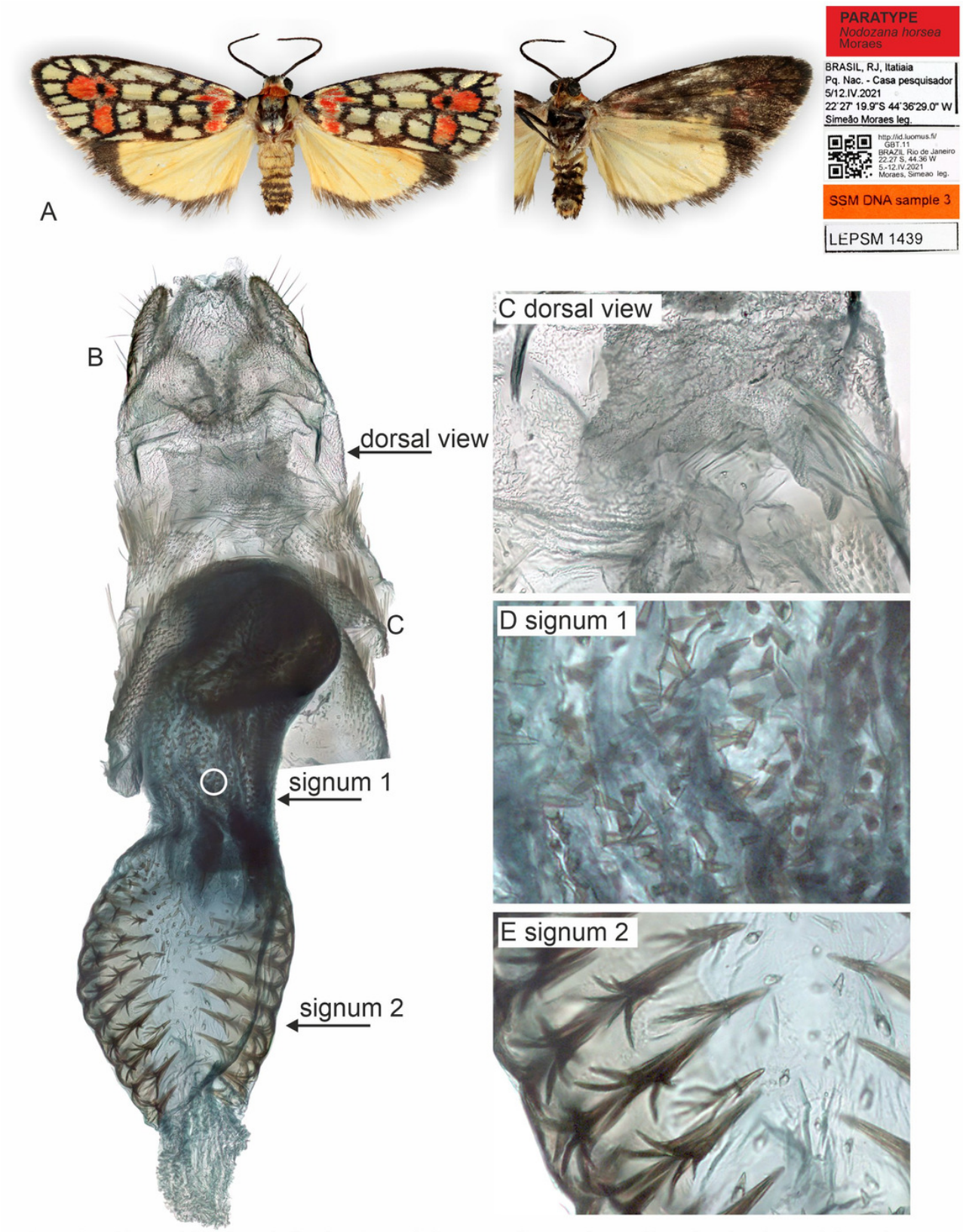

Figure 3. Habitus and female genitalia of *Nodozana helia* **sp. nov.** (paratype). A. Habitus, dorsal and ventral view, wingspan 18 mm. B. Female genitalia, ventral view, point of origin of ductus seminalis indicated with circle. C. Detail of pheromone grland, dorsal view. D. Detail of signum on posterior portion of corpus bursae. E. Detail of signum on anterior portion of corpus bursae. All genitalia pictures from dissection SMM516.

Figure 4

Habitus and male genitalia of *Epeiromulona pataxo* Moraes & Aguiar sp. nov. (paratype)

A. Habitus, dorsal and ventral view, wingspan 13 mm. B. Genital capsule, ventral view. C. Aedeagus, lateral view. D. Aedeagus with everted vesica, lateral view. E. Genital capsule with aedeagus, lateral view. F. Detail of micro spicules at apex of aedeagus.

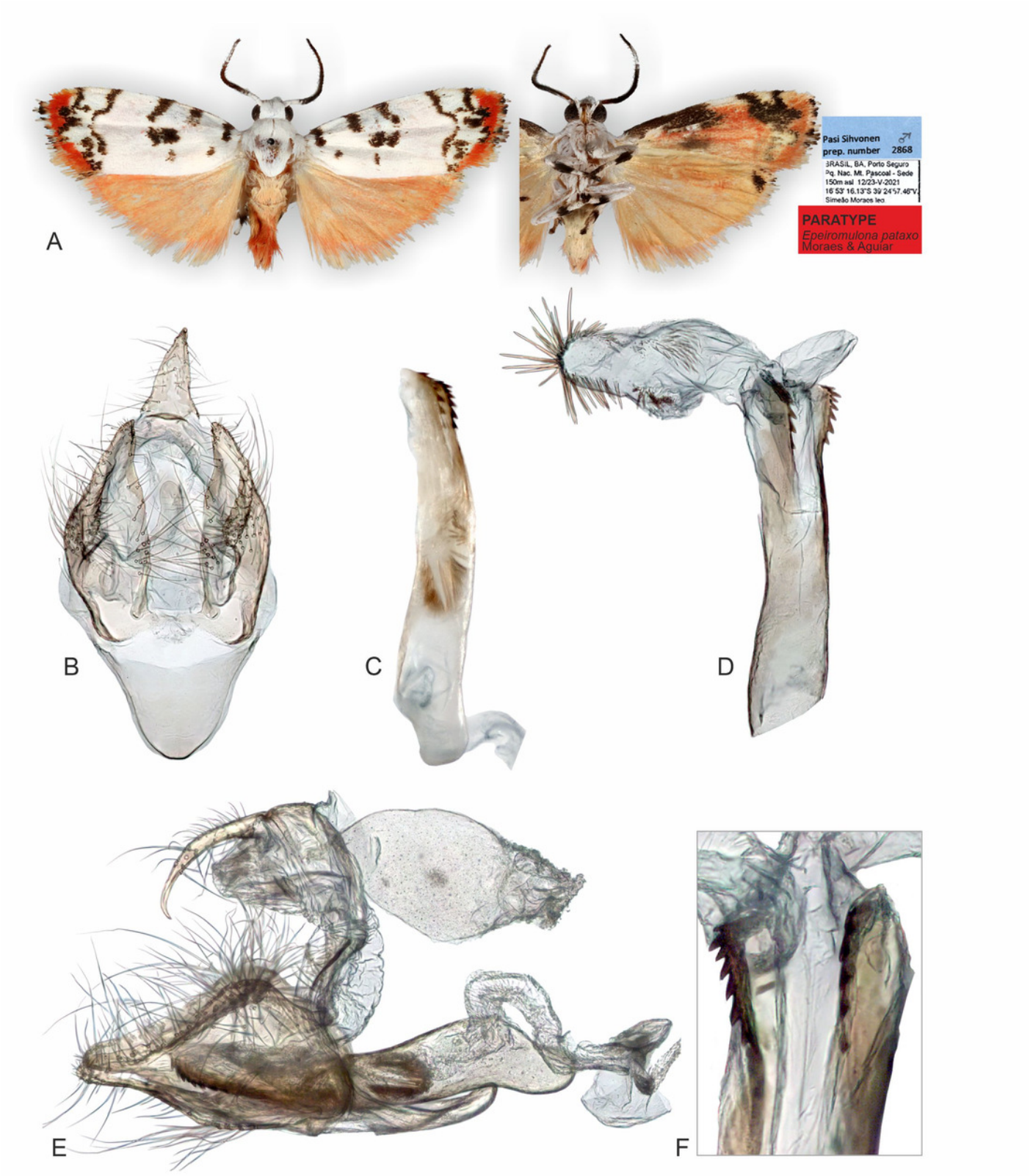

Figure 4. Habitus and male genitalia of *Epeiromulona pataxo* Moraes & Aguiar **sp. nov.** (paratype). A. Habitus, dorsal and ventral view, wingspan 13 mm. B. Genital capsule, ventral view. C. Aedeagus, lateral view. D. Aedeagus with everted vesica, lateral view. E. Genital capsule with aedeagus intact, lateral view. F. Detail of micro spicules at apex of aedeagus.

Figure 5

Habitus and female genitalia of *Epeiromulona pataxo* Moraes & Aguiar sp. nov. (paratype)

A. Habitus, dorsal and ventral view, wingspan 14 mm. B. Female genitalia, ventral view (point of origin of ductus seminalis indicated with circle). C. Detail of signum on posterior portion of corpus bursae. D. Detail of signum on anterior portion of corpus bursae.

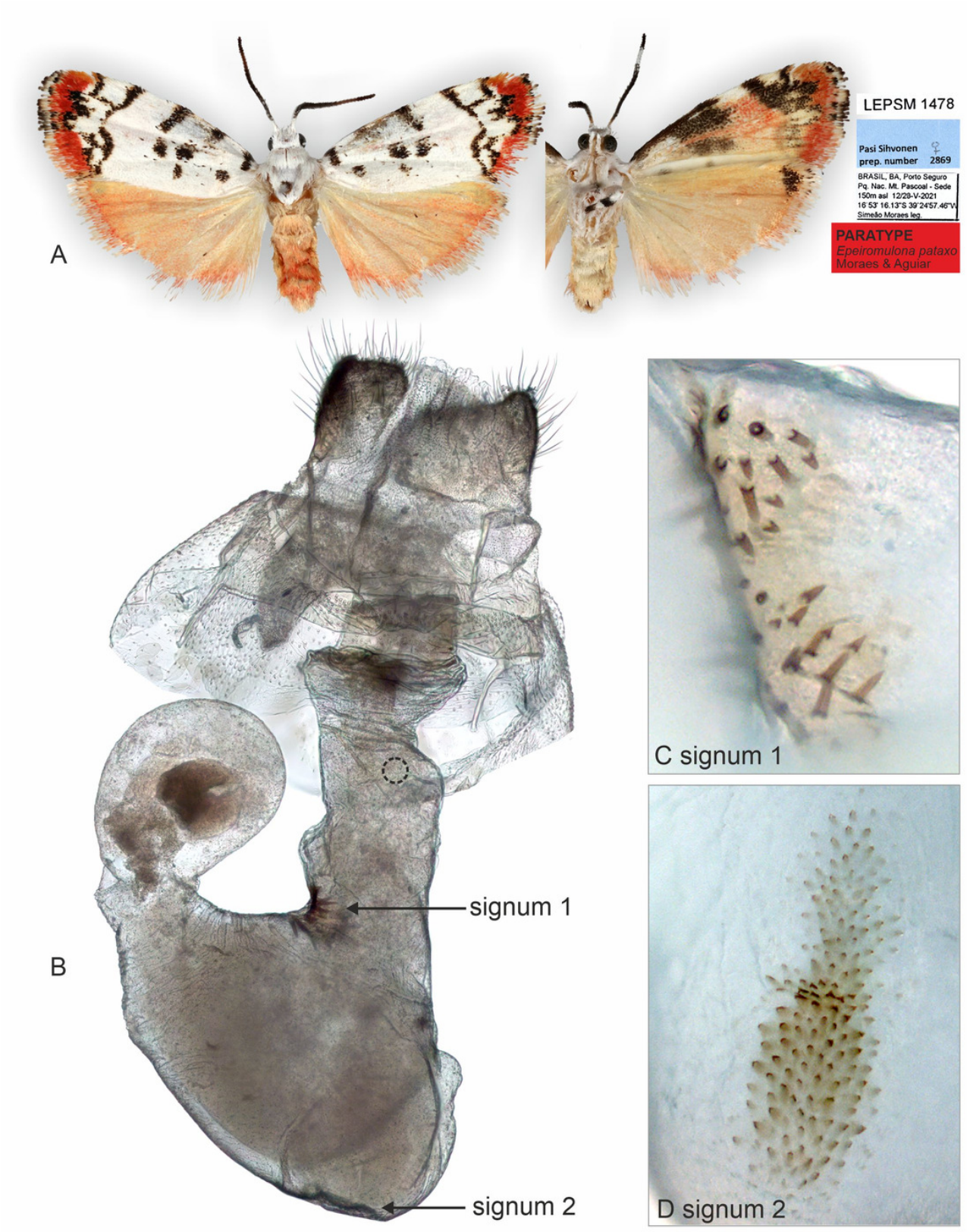

Figure 5. Habitus and female genitalia of *Epeiromulona pataxo* Moraes & Aguiar **sp. nov.** (paratype). A. Habitus, dorsal and ventral view, wingspan 14 mm. B. Female genitalia, ventral view (point of origin of ductus seminalis indicated with circle). C. Detail of signum on posterior part of corpus bursae. D. Detail of signum on anterior portion of corpus bursae.

Figure 6

Micro-CT images of male genitalia of *Nodozana heliae* Moraes sp. nov. (paratype)

A-D**.** Images from the 3D model in different angles. E-F. Structures from different angles as indicated. E. Posterior margin of 8th sternite, transtilla, anterior margin of valva highlighted, protractors muscles of aedeagus marked in green. F. Margins of uncus, tegumen and valva highlighted, flexor muscle of uncus marked with green. G. Margin of valva and subscaphium highlighted, flexor muscle of valva and retractor muscle of aedeagus marked with green. H. Margins of aedeagus and cornutus highlighted, retractors muscles of aedeagus marked in green.

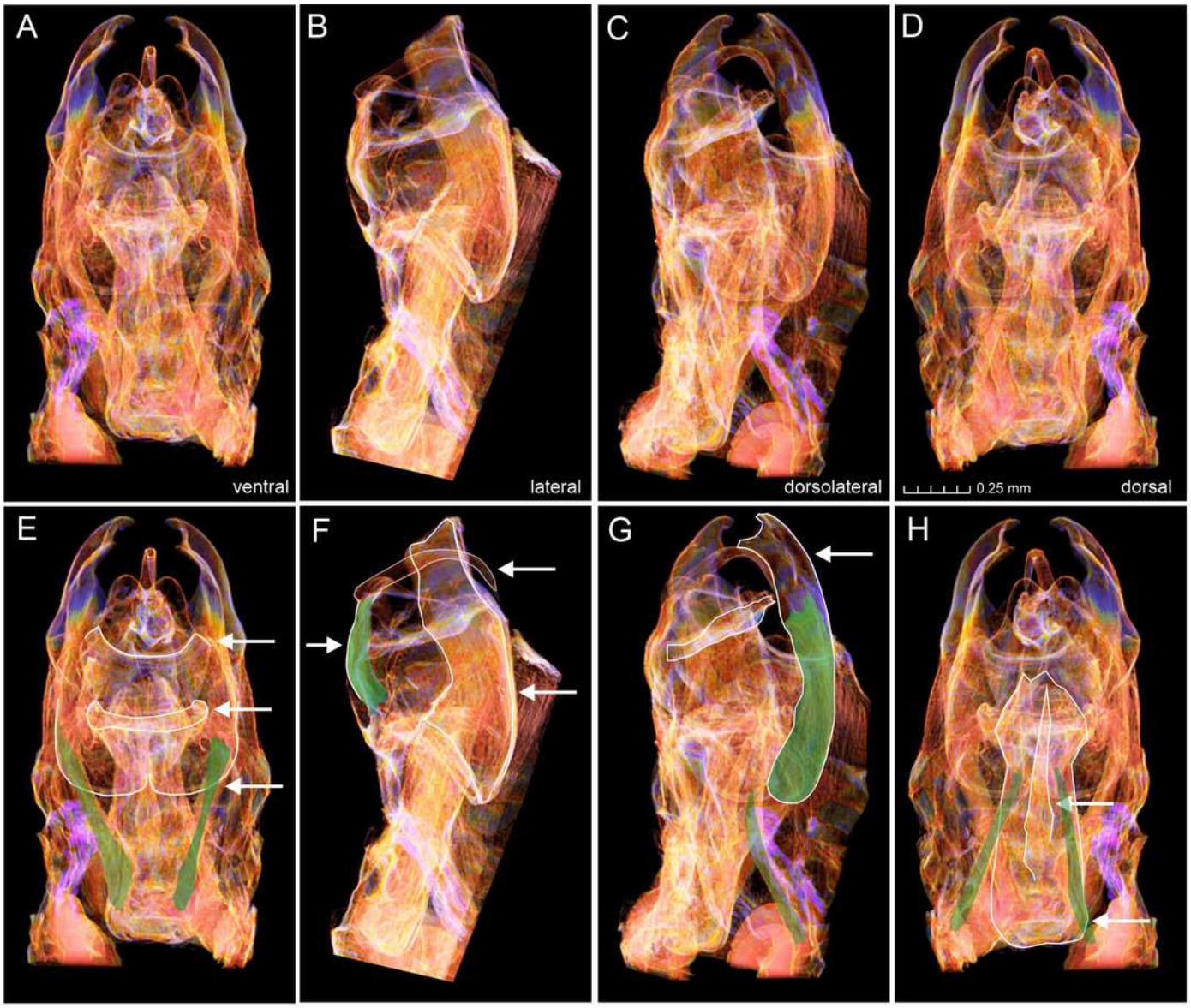

Figure 6. Micro-CT images of male genitalia of *Nodozana helia* **sp. nov.** from different angles. A-D. Images from 3D model in different angles. E-F. Selected structures from different angles as indicated. E. Posterior margin of 8th sternite, transtilla and anterior margin of valva highlighted. F. Margins of uncus, tegumen and valva highlighted, flexor muscle of uncus marked with green. G.Margin of valva highlighted, flexor muscle of valva marked with green. H. Margins of aedeagus and cornutus highlighted.

Figure 7

Sagittal slices from 3D model of female genitalia of *Nodozana heliae* Moraes sp. nov. (paratype).

A-H. Slices showing margin of sclerotized and membranous structures. CB: corpus bursae, DB: ductus bursae, PA: papillae anales, PhGl: pheromone gland, OB: ostium bursae, SG1: signum 1, SG2: signum 2.

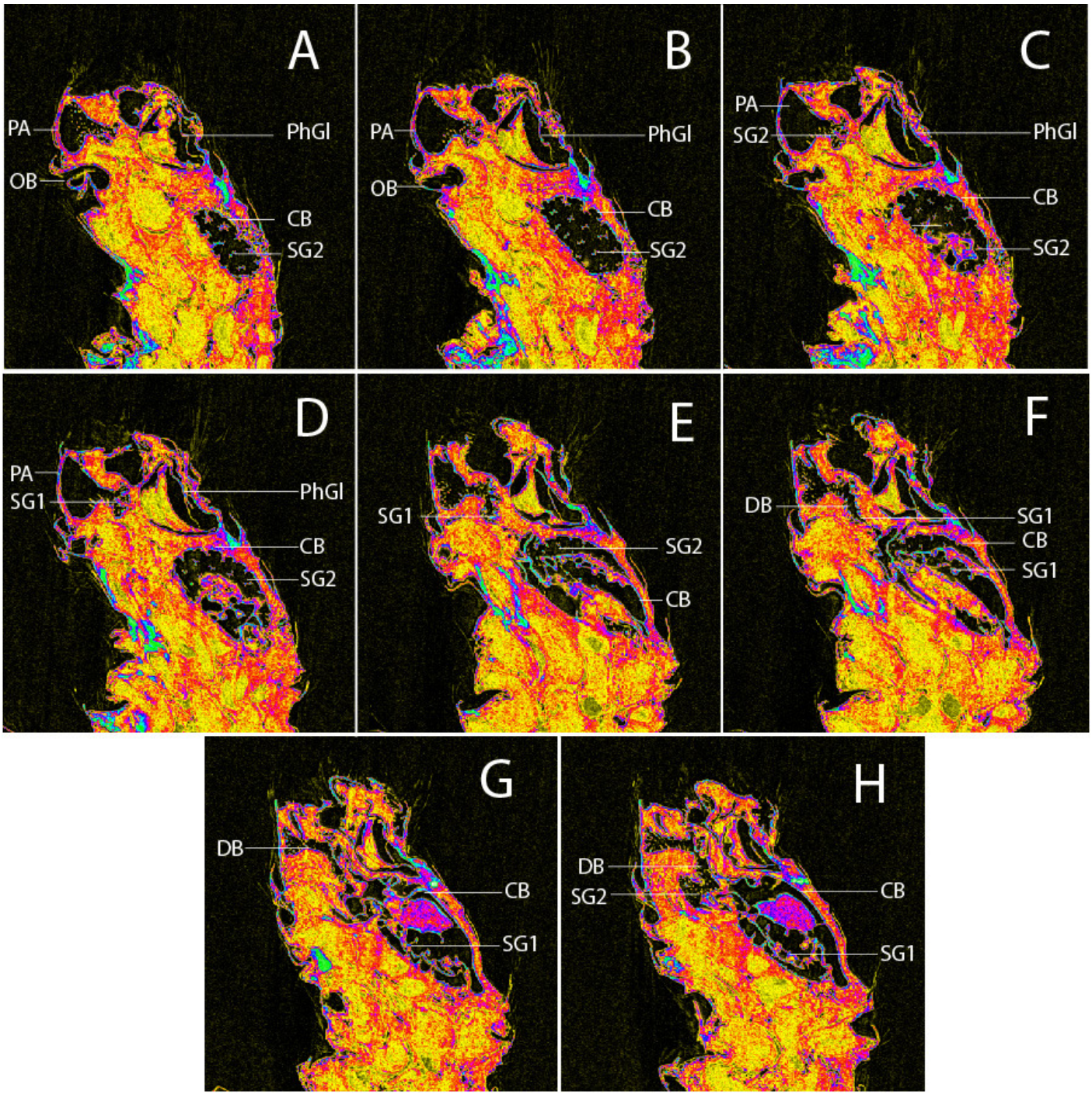
A
PA
PhGl
OB
CB
SG2
B
PA
PhGl
OB
CB
SG2
C
PA
SG2
PhGl
CB
SG2
D
PA
SG1
PhGl
CB
SG2
E
SG1
SG2
CB
F
DB
SG1
CB
SG1
G
DB
CB
SG1
H
DB
SG2
CB
SG1